

Parafermions in a multilegged geometry: Towards a scalable parafermionic networkUdit Khanna ^{1,2,*}, Moshe Goldstein ¹ and Yuval Gefen²¹*Raymond and Beverly Sackler School of Physics and Astronomy, Tel Aviv University, Tel Aviv 6997801, Israel*²*Department of Condensed Matter Physics, Weizmann Institute of Science, Rehovot 76100, Israel* (Received 9 September 2021; revised 26 March 2022; accepted 30 March 2022; published 12 April 2022)

Parafermionic zero modes are non-Abelian excitations which have been predicted to emerge at the boundary of topological phases of matter. Contrary to earlier proposals, here we show that such zero modes may also exist in multilegged star junctions of quantum Hall states. We demonstrate that the quantum states spanning the degenerate parafermionic Hilbert space may be detected and manipulated through protocols employing quantum antidots and fractional edge modes. Such star-shaped setups may be the building blocks of two-dimensional parafermionic networks.

DOI: [10.1103/PhysRevB.105.L161101](https://doi.org/10.1103/PhysRevB.105.L161101)

Introduction. Parafermion (PF) zero modes are fractionalized excitations with non-Abelian statistics, which may exist at the boundary of certain topological phases of matter [1]. PF zero modes are expected to show a number of interesting phenomena [2–21] such as the fractional Josephson effect, zero-bias anomaly, and topological Kondo effect, and may be potentially useful in quantum information applications [5,22–30]. General classifications of truly one-dimensional (1D) bosonic and fermionic systems rule out the existence of PFs beyond Majorana zero modes [31–34]. However, PF zero modes may be supported at suitably designed line junctions at the boundary of fractional quantum Hall (QH) states [2–4]. In particular, two counterpropagating chiral edge modes with opposite spins, at the interface of fractional quantum Hall (FQH) puddles in the $\nu = 1/m$ state, may be gapped by proximity to a bulk superconductor or a ferromagnet. The domain walls between superconducting and ferromagnetic segments are expected to host \mathbb{Z}_{2m} PF zero modes on the boundary [2,3]. Similar setups have been proposed for the $\nu = 2/3$ state [5], in hierarchical [35] and bilayer [36–38] fractional QH phases, in proximitized and fractional topological insulators [11,20,39–44], as well as in systems of coupled 1D wires [45–52]. Such PF modes can be detected through their transport signatures in appropriately designed setups [7,19,21,38,53,54]. Two-dimensional parafermionic networks are predicted to host even more exotic Fibonacci anyons, which may eventually allow fault-tolerant universal quantum computation [5,6,55,56].

Here we propose a setup hosting PF zero modes, based on multilegged star junctions of FQH states. Figure 1 shows the simplest such geometry supporting a parafermionic zero mode localized at the center of the star junction. Such a geometry may be based on single-layer FQH states [2,3] employing superconducting regions [Fig. 1(a)] or double-layer states [36,37] employing interlayer electron tunneling at the

interfaces [Fig. 1(b)]. Similar setups have been studied previously in the context of Majorana zero modes (which are \mathbb{Z}_2 PFs) localized at the boundaries of 1D nanowires [57–65]. These studies found that a single zero-energy Majorana mode is supported at the center of odd-legged star junctions, but not in the case of an even number of legs. The present work is a concrete extension of the previous studies to the case of $m > 1$ PF modes, which requires one to consider interacting systems. Here, one might naively expect a modulo $2m$ dependence on the number of wires. In contrast, we interestingly find the modulo 2 behavior to persist, namely, that parafermionic junctions with an odd (even) number of legs would (would not) host a single parafermion at the center of the star which cannot (can) be gapped out. Below we analyze the low-energy dynamics of a trijunction geometry, demonstrating the existence of parafermionic zero mode and the degeneracy of the zero-energy Hilbert space. Furthermore, we propose specific setups employing quantum antidots (QADs) and fractional edge modes, which may be used to measure the degeneracy of the parafermionic Hilbert space and facilitate manipulation of such states.

Trijunction model. We consider a single trijunction setup [Fig. 1(a)] comprising the boundary of three $\nu_j = \nu = \frac{1}{m}$ ($j = 1, 2, 3$) QH puddles with same spin polarization. The low-energy dynamics of each puddle is governed by a chiral edge mode, described by a bosonic field $\phi_j(x, t)$ [66]. These bosonic fields are described by the Hamiltonian

$$H_{\text{edge}} = \frac{mv}{4\pi} \sum_{j=1}^3 \int dx [\partial_x \phi_j(x)]^2, \quad (1)$$

where v is the edge mode velocity (assumed to be identical, for all puddles, for simplicity) and satisfy

$$[\phi_j(x), \phi_j(y)] = \frac{i\pi}{m} \text{sgn}(x - y), \quad (2)$$

$$[\phi_j(x), \phi_k(y)] = i\frac{\pi}{m} \text{ for all } j > k. \quad (3)$$

*Present address: Department of Physics, Bar-Ilan University, Ramat Gan 52900, Israel; udit.khanna.10@gmail.com

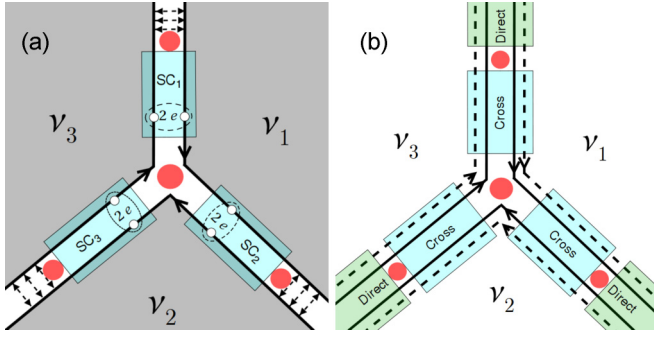


FIG. 1. Trijunctions hosting parafermionic zero modes (represented by red circles) may be constructed in (a) single-layer or (b) double-layer setups. The black lines represent the chiral edge modes of the three quantum Hall puddles. In (b), the solid (dashed) lines represent the edge modes of the top (bottom) layer. Counterpropagating pairs of edge modes may be gapped out by introducing superconducting or electron-tunneling segments in the single-layer setup [panel (a)]. In the bilayer setup [panel (b)], edge modes may be gapped out by introducing segments with direct (intralayer) or crossed (interlayer) electron tunneling.

Here the coordinate x increases along the direction of propagation for each edge mode. The second commutator above relies on the assumption that the edge modes are segments of a single boundary. At the center of the trijunction, each pair of counterpropagating edge modes is gapped out through proximity coupling to a p -wave superconductor [67]. The superconducting regions are described by

$$H_s = \Delta \sum_j \int dx \cos[m(\phi_j + \phi_{j-1}) + \hat{\phi}], \quad (4)$$

where ϕ_0 has been identified with ϕ_3 , and we assume the amplitude (Δ) and phase ($\hat{\phi}$) of all superconducting segments to be identical. This is possible if all three segments are generated by proximity to the same bulk superconductor. In order to fix the boundary conditions and the total charge hosted by the setup, we also assume that (away from the junction) each pair of counterpropagating modes is gapped out through strong interedge electron tunneling [denoted as black dashed double-headed arrows in Fig. 1(a)]. The tunneling regions are described by

$$H_t = g \sum_j \int dx \cos[m(\phi_j - \phi_{j-1})]. \quad (5)$$

Finally, we assume that the superconducting segments (implicitly assumed to be part of the same bulk superconductor) are floating. Their total charge (Q_T) appears in the Hamiltonian as a charging term, $(\hat{Q} - Q_T)^2/2C$, where $\hat{Q} = \sum_j \hat{Q}_j$ is the total charge and \hat{Q}_j is the charge hosted in the j th superconducting segment, and is given by

$$\hat{Q}_j = \frac{1}{2\pi} \int_{SC_j} dx (\partial_x \phi_j - \partial_x \phi_{j-1}). \quad (6)$$

Since the (total) charge and phase of the superconductor are conjugate variables, they satisfy $[\hat{\phi}, \hat{Q}] = 2i$.

We restrict our analysis to energies below $\sqrt{4\pi mv\Delta}$ and $\sqrt{4\pi mv g}$. In this limit, the fractional chirals may be assumed

to be completely pinned inside the superconducting and tunneling segments [3]. It follows that the superconducting and tunneling regions are described by integer-valued operators \hat{N}_j and \hat{M}_j , respectively. Therefore at each boundary of the trijunction, we must have

$$\phi_j + \phi_{j-1} = \frac{2\pi}{m} \hat{N}_j, \quad (7)$$

where $\hat{N}_j \rightarrow \hat{N}_j + \hat{\phi}/m$. Similarly, at each boundary of the tunneling regions we have

$$\phi_j - \phi_{j-1} = \frac{2\pi}{m} \hat{M}_j. \quad (8)$$

Our next task is to analyze the low-lying dynamics of this trijunction block showing that it exhibits parafermionic physics. To this end, we perform a standard mode expansion of the chiral fields,

$$\begin{aligned} \phi_j(x, t) = & \varphi_j + A_j p_{\varphi_j}(vt - x) \\ & + \sum_{n>0} [B_{nj} a_{nj} e^{-iq_n(vt-x)} + \text{H.c.}], \end{aligned} \quad (9)$$

where A_j and B_{nj} are c numbers and a_{nj} describe the bosonic excitations in the chiral modes. Imposing the boundary conditions [Eq. (7)] and commutation relation [Eq. (2)] inside the trijunction, we find

$$\phi_1(x, t) = \varphi_1 + \sqrt{\frac{2}{m}} \sum_{n>0} \left[\frac{a_n}{\sqrt{2n-1}} e^{-iq_n(vt-x)} + \text{H.c.} \right], \quad (10)$$

$$\phi_2(x, t) = -\phi_1(x + L_1, t) + \varphi_1 + \varphi_2, \quad (11)$$

$$\phi_3(x, t) = -\phi_2(x + L_2, t) + \varphi_2 + \varphi_3, \quad (12)$$

where $\varphi_j = \frac{\pi}{m}(\hat{N}_j + \hat{N}_{j+1} - \hat{N}_{j-1})$ (not to be confused with $\hat{\phi}$), $q_n = (2n-1)\frac{\pi}{\ell}$, L_j is the length of the j th chiral inside the trijunction, and $\ell = \sum_j L_j$. A similar expansion can be performed for the region between the superconductor and the tunneling segments [2].

Plugging the expansion found above into Eq. (3), we find that the only nonzero commutation relations are

$$[\hat{N}_3, \hat{N}_2] = \frac{im}{\pi} \quad \text{and} \quad (13)$$

$$[\hat{N}_1, \hat{M}_1] = [\hat{N}_2, \hat{M}_1] = [\hat{N}_3, \hat{M}_1] = \frac{im}{\pi}. \quad (14)$$

Using (6), the charge on the superconducting segments (at low energies) is found to be

$$\hat{Q}_j = \frac{1}{m} (\hat{N}_{j+1} - \hat{N}_{j-1} - \hat{M}_j). \quad (15)$$

Note that the total charge $\hat{Q} = -\sum_j \hat{M}_j$ depends only on the integers describing the electron-tunneling regions at the boundaries. Since the charge on each superconducting segment is defined module 2, the physical operators to consider are $e^{i\pi \hat{Q}_j}$. These satisfy

$$e^{i\pi \hat{Q}_j} e^{i\pi \hat{Q}} = e^{i\pi \hat{Q}} e^{i\pi \hat{Q}_j} \quad \text{and} \quad (16)$$

$$e^{i\pi \hat{Q}_{j-1}} e^{i\pi \hat{Q}_j} = e^{i(\pi/m)} e^{i\pi \hat{Q}_j} e^{i\pi \hat{Q}_{j-1}} \quad \text{for all } j. \quad (17)$$

Finally, we may write the Hamiltonian of the trijunction (ignoring the charging term for now) as

$$H = H_{\text{edge}} + H_s + H_t = \sum_{n>0} vq_n \left(a_n^\dagger a_n + \frac{1}{2} \right). \quad (18)$$

Note that H only depends on the bosonic excitations of the chiral fields and not on \hat{N} . This allows for the possibility that the Hamiltonian supports zero-energy solutions. To this end, we construct operators which commute with the Hamiltonian and describe (local) superpositions of quasiholes and quasiparticles in the chiral edge modes. A quick calculation confirms that the operator $\tilde{\Gamma}$ defined as

$$\tilde{\Gamma}_0 = e^{i\varphi_1} \int dx \sum_{k=1}^3 [e^{-i\varphi_k} e^{i\phi_k(x)} + \text{H.c.}] \quad (19)$$

satisfies these requirements [68]. We may define $\Gamma_0 = e^{i\varphi_1} = e^{i(\pi/m)(\hat{N}_1 + \hat{N}_2 - \hat{N}_3)}$ as the projection of $\tilde{\Gamma}_0$ onto the ground state (in the absence of bosonic fluctuations). Similar expressions can be defined for the three zero modes (Γ_j) localized at the domain wall between the (j th) superconducting segment and corresponding tunnel junction at the boundary of the trijunction. Therefore the low-energy physics of the trijunction is governed by the four localized zero-energy modes which satisfy parafermionic commutation relations, $\Gamma_\alpha \Gamma_\beta = e^{i(\pi/m)} \Gamma_\beta \Gamma_\alpha$ if α appears to the left of β in the tuple (1, 0, 2, 3). We note that there are multiple ways to represent the PF zero modes, which are localized at the different boundaries of the junction (for instance, Γ_0 as defined above is localized at ϕ_1). Here we have used the convention that Γ_j ($j = 1, 2, 3$) is localized at ϕ_j .

The low-energy subspace of the trijunction is expected to be degenerate due to the PF commutation relations of the zero modes. Since the operators $e^{i\pi\hat{Q}_j}$ commute with H , the different states in the ground state sector may be labeled through their eigenvalues. The nontrivial commutations among these operators imply that the Hilbert space is spanned by states of the form $|Q_T, Q_j\rangle$ (for a fixed j). Since $e^{i\pi\hat{Q}_j}$ can assume $2m$ values, the total degeneracy of the ground state of the trijunction is $(2m)^2$, which is consistent with the presence of four \mathbb{Z}_{2m} PF modes. Note that the energy of states with different Q_T is set externally through the charging term in the Hamiltonian [which was ignored in Eq. (18)]. Therefore the degeneracy of such states is lifted for finite charging energy. By contrast, the $2m$ states with a given Q_T are degenerate up to exponentially small splittings (arising from the finite length of the superconductor) [69] which are neglected here.

Our analysis of the trijunction may be extended to star-shaped setups with a larger number of legs. The results are qualitatively unaltered for stars with an odd number of legs. On the other hand, for even-legged junctions, the low-energy Hamiltonian of the junction [H in Eq. (18)] involves additional terms which explicitly depend on the integer-valued operators \hat{N}_j . Such terms rule out the possibility of a \mathbb{Z}_{2m} PF zero mode at the center of an even-legged junctions. Our results are also applicable to star-shaped junctions in bilayer setups. Specifically, a trijunction comprising the edge of the QH bilayer [Fig. 1(b)] with $\nu = 1/m$ per layer would host a \mathbb{Z}_m PF zero mode at its center.

Ground state manipulation. Here we discuss protocols (adopted from Ref. [53]) to induce transitions between the degenerate low-energy states of the trijunction. As described above, the total charge of the trijunction (Q_T) is fixed externally through the charging energy. However, the degenerate states within a topological sector (labeled by Q_T), may be manipulated through redistribution of the charge among the superconducting segments. Suppose $|\Psi\rangle$ is an eigenstate of $e^{i\pi\hat{Q}_1}$ with eigenvalue $e^{i\pi Q_1} = 1$; Eqs. (1) and (16) then imply that $(e^{i\pi\hat{Q}_2})^k |\Psi\rangle$ is also an eigenstate of $e^{i\pi\hat{Q}_1}$ with eigenvalue $e^{i(\pi k/m)}$. Therefore one may induce transitions between $|Q_T, Q_1\rangle$ and $|Q_T, Q_1 + \frac{1}{m}\rangle$ through the application of $e^{i\pi\hat{Q}_2}$. Similarly, application of $e^{i\pi\hat{Q}_3}$ induces transitions from $|Q_T, Q_1\rangle$ to $|Q_T, Q_1 - \frac{1}{m}\rangle$.

Figure 2 depicts several setups involving two QADs coupled to the trijunction, which may be used to apply the operators $e^{i\pi\hat{Q}_j}$. We assume that each QAD may be empty or host a single Laughlin quasiparticle depending on the voltage applied. Thus, effectively each QAD can be modeled by a two-level system with the Hamiltonian,

$$H_{\text{QAD}} = V_Q \left(N_\psi - \frac{1}{2} \right), \quad (20)$$

where V_Q is proportional to the electrostatic potential on the QAD and N_ψ is the number of quasiparticles in the QAD. The tunnel coupling of the QADs to the PF modes in the trijunction may be described by

$$H_{\text{tun}} = \sum_{k=1,2} \tilde{J}_k \psi_k \Gamma_k^\dagger + \text{H.c.}, \quad (21)$$

where ψ_k is the quasiparticle operator for the k th QAD satisfying $[N_{\psi_k}, \psi_k] = -\psi_k$, and Γ_k is the PF operator coupled to the QAD. Since the PF modes have multiple representations (which are localized at different edges), here Γ_k is assumed to be localized at the boundary of the QH region in which the QAD is located. We assume that the tunneling amplitudes (\tilde{J}_k) are much smaller than the charging energy of the trijunction (E_c) so that H_{tun} leads to cotunneling of quasiparticles between the QADs, which may be described by

$$H_{\text{co-tun}} = J \psi_1 \psi_2^\dagger \Gamma_1^\dagger \Gamma_2 + \text{H.c.} \quad (22)$$

Here $J \sim \tilde{J}_1 \tilde{J}_2^* / E_c$ for $E_c \gg \tilde{J}_{1,2}$. Let us assume that the QADs were initially decoupled from the trijunction and prepared such that one QAD is occupied while the other is empty. Then by coupling them to the trijunction and slowly varying the voltage on the dots, we may induce the transition $|\Psi\rangle \rightarrow \Gamma_1^\dagger \Gamma_2 |\Psi\rangle$. Using Eqs. (13)–(15), we find that the terms of the form $\Gamma_0 \Gamma_j^\dagger$ are proportional to the operators $e^{i\pi\hat{Q}_j}$. We may facilitate the application of any operator ($e^{i\pi\hat{Q}_j}$) through suitable placement of the two QADs. The setups shown in Figs. 2(a)–2(c) may be used to realize $e^{i\pi\hat{Q}_1}$, $e^{i\pi\hat{Q}_2}$, and $e^{i\pi\hat{Q}_3}$, respectively.

Degeneracy of parafermionic states. For a given total charge (Q_T), the degeneracy of the low-energy Hilbert space of the trijunction is expected to be $2m$. Here we propose a setup (depicted in Fig. 3), involving QADs and two external fractional QH edge modes, to directly observe the degenerate subspace. The external fractional modes act as leads from

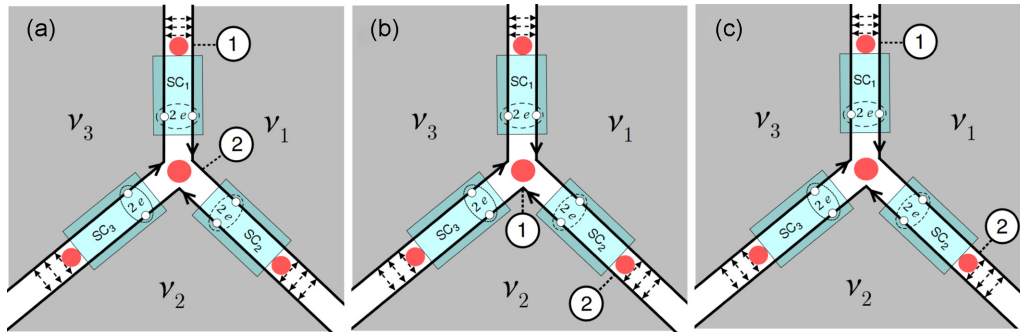


FIG. 2. Schemes for state manipulation in the trijunction (adopted from Ref. [53]). The white circles denote quantum antidots which may host a single Laughlin quasiparticle and are tunnel coupled to one of the interfaces supporting a parafermionic mode. As described in the text, the state of the trijunction may be manipulated through the application of operators of the form $e^{\pm i\pi\hat{Q}_j}$ ($j = 1, 2, 3$). Varying the gate voltage on the antidots in an adiabatic fashion allows for the application of (a) $e^{\pm i\pi\hat{Q}_1}$, (b) $e^{\pm i\pi\hat{Q}_2}$, and (c) $e^{\pm i\pi(\hat{Q}_1+\hat{Q}_2)} \sim e^{\pm i\pi(\hat{Q}-\hat{Q}_3)}$. Moving the antidots to the opposite side of the same interface would modify the operator by an overall phase.

which fractional quasiparticles may tunnel into the trijunction. The Hamiltonian of the two edge modes is given by $H_a = (mv/4\pi) \int dx [\partial_x \phi_a]^2 - V_a \int dx \partial_x \phi_a$, where V_a is the voltage on ϕ_a ($a = s, d$). The quasiparticle tunneling from the edges to the trijunction is described by

$$H_{\text{qp}} = \sum_{a=s,d} \tilde{\eta}_a e^{i\phi_a} \Gamma_a^\dagger + \text{H.c.} \quad (23)$$

As pointed out above, the representation of the PF mode has to be appropriately chosen so that fractional charge only tunnels across the bulk of a QH state, and not across vacuum. If the charging energy for the trijunction is large, then only cotunneling processes are allowed at low energies. These are described by $H_{\text{ct}} = \eta_c \Gamma_1 \Gamma_0^\dagger e^{-i\phi_d} e^{i\phi_s} + \text{H.c.}$, where Γ_0 is the PF located inside the trijunction and Γ_1 is the PF located at a domain wall between a superconductor and tunneling

segment (cf. Fig. 3). We assume that quasiparticles may also tunnel between the two modes directly (without involving the trijunction). Such processes are described by $H_{\text{dir}} = \eta_d e^{-i\phi_d} e^{i\phi_s} + \text{H.c.}$. Then the total tunneling Hamiltonian is $H_{\text{dir}} + H_{\text{ct}} = (\eta_d + \eta_c \Gamma_1 \Gamma_0^\dagger) e^{-i\phi_d} e^{i\phi_s} + \text{H.c.}$, which induces a finite current from the source S to the drain D in Fig. 3. The tunneling current may be evaluated in the limit of weak tunneling, following the analysis of Wen [70], as

$$I_t = \frac{|\eta_{\text{eff}}|^2}{v^{2\nu}} \frac{2\pi\nu}{\Gamma(2\nu)} (\nu|V_1 - V_2|)^{2\nu-1}, \quad (24)$$

where η_{eff} is the eigenvalue of $\eta_d + \eta_c \Gamma_1 \Gamma_0^\dagger$. As shown earlier, the operator $\Gamma_j \Gamma_0^\dagger$ depends on $e^{i\pi\hat{Q}_j}$ ($e^{i\pi\hat{Q}_1}$ for the setup in Fig. 3). This implies that the current I_t between the edge modes is sensitive to the state of the trijunction, which may be labeled using $e^{i\pi\hat{Q}_1}$. In fact, the state of the trijunction would be projected to an eigenstate of $e^{i\pi\hat{Q}_1}$ upon measurement of the tunneling current (I_t).

The QADs in the setup shown in Fig. 3 may be used to apply the operator $e^{i\pi\hat{Q}_2}$ to the state of the trijunction, which induces a transition between the degenerate states labeled by $e^{i\pi\hat{Q}_1}$. As discussed above, the tunneling current I_t is expected to change after the application of $e^{i\pi\hat{Q}_2}$, as it depends on the state of the trijunction. Therefore, the degeneracy of the trijunction (for a given charge Q_T) may be measured by repeatedly monitoring I_t and applying $e^{i\pi\hat{Q}_2}$ through the QADs. The number of steps required before I_t returns to its initial value is the number of degenerate states in the PF Hilbert space.

Prospects of parafermionic networks. The PF zero modes, hosted at the center of star junctions, are identical to those realized in line junction setups [2,3]. However, a crucial advantage of our proposal is that such junctions may be used as building blocks for constructing complex parafermionic networks. We first note that the connectivity of a single trijunction, depicted in Fig. 1, is higher than the case of a four PF line junction. Such a configuration could be useful for implementing complex operations (such as, braiding [24]) on the PF modes. Going on to a small number of star junctions may be combined in a myriad of configurations, each of which may

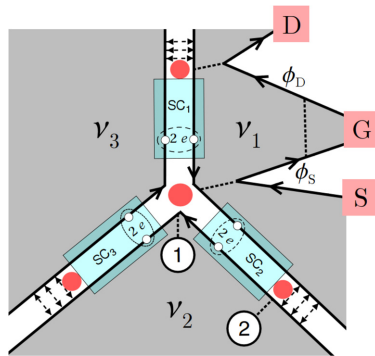


FIG. 3. Scheme for measuring the degeneracy of the trijunction (adopted from Ref. [53]). The white circles denote quantum antidots which facilitate the application of $e^{\pm i\pi\hat{Q}_2}$ upon the trijunction state. $\phi_{S/D}$ are additional fractional edge modes tunnel coupled to the trijunction and to each other. Quasiparticles emanated from the source (S) may end up at the drain (D), by directly tunneling from ϕ_s to ϕ_d , or by tunneling across the trijunction. The interference between these two processes, and therefore the current (I_t) from S to D, is sensitive to the state of the trijunction. Therefore repeatedly applying $e^{i\pi\hat{Q}_2}$ through the antidots and monitoring I_t , allows one to measure the number of degenerate states in the parafermionic Hilbert space of the trijunction (for a fixed total charge).

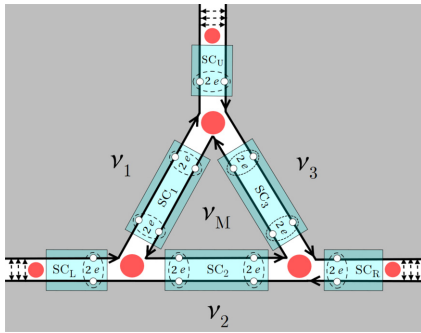


FIG. 4. Multiple trijunctions may be connected to form complex parafermionic networks. The figure depicts a combination of three trijunctions, with a quantum Hall island enclosed only by parafermionic zero modes.

be useful for easily implementing a different set of operations. Figure 4 depicts one such configuration involving three trijunctions, which involves a QH island surrounded only by PF zero modes. Repeating the mode expansion analysis for such *loop* geometries, we find that the PF states are sensitive to the fractional charge in the bulk of the enclosed QH puddle, which in turn may be manipulated through additional QADs. Configurations involving several such loops could be useful for quantum information applications. Finally, several such junctions may be employed for constructing large PF networks with different topologies, such as a cycle-free Bethe lattice or a two-dimensional honeycomb structure. The braiding properties of PFs moving on such networks depend sensitively on

their connectivity [71–73]. Additionally at low energies, such networks may be described in terms of emergent phases that support even more exotic non-Abelian excitations [5].

Conclusions. We have demonstrated that setups involving multilegged star junctions of fractional quantum Hall states, may serve as a platform which hosts parafermionic zero modes. Specifically, employing a low-energy mode expansion, we showed that a star with odd (even) number of legs supports (does not support) a parafermionic mode at its center. We also proposed setups involving additional quantum antidots and fractional edge modes, which facilitate the detection and manipulation of the parafermionic states. The star-shaped junction proposed here, could be used as building blocks for constructing complex parafermionic networks, including two-dimensional lattices, which may be quite difficult to realize using just line junctions. A detailed investigation of the emergent physics of such networks is left for the future.

Acknowledgments. We acknowledge useful discussions with Kyrylo Snizhko. U.K. was supported by the Raymond and Beverly Sackler Faculty of Exact Sciences at Tel Aviv University and by the Raymond and Beverly Sackler Center for Computational Molecular and Material Science. M.G. was supported by the US-Israel Binational Science Foundation (Grant No. 2016224). Y.G. was supported by CRC 183 (project C01), the Minerva Foundation, DFG Grants No. RO 2247/11-1 and No. MI 658/10-1, the German Israeli Foundation (Grant No. I-118-303.1-2018), the Helmholtz International Fellow Award, and by the Italia-Israel QUANTRA grant.

- [1] J. Alicea and P. Fendley, Topological phases with parafermions: Theory and blueprints, *Annu. Rev. Condens. Matter Phys.* **7**, 119 (2016).
- [2] D. J. Clarke, J. Alicea, and K. Shtengel, *Nat. Commun.* **4**, 1348 (2013).
- [3] N. H. Lindner, E. Berg, G. Refael, and A. Stern, Fractionalizing Majorana Fermions: Non-Abelian Statistics on the Edges of Abelian Quantum Hall States, *Phys. Rev. X* **2**, 041002 (2012).
- [4] L. H. Santos and T. L. Hughes, Parafermionic Wires at the Interface of Chiral Topological States, *Phys. Rev. Lett.* **118**, 136801 (2017).
- [5] R. S. K. Mong, D. J. Clarke, J. Alicea, N. H. Lindner, P. Fendley, C. Nayak, Y. Oreg, A. Stern, E. Berg, K. Shtengel, and M. P. A. Fisher, Universal Topological Quantum Computation from a Superconductor-Abelian Quantum Hall Heterostructure, *Phys. Rev. X* **4**, 011036 (2014).
- [6] J. Alicea and A. Stern, Designer non-Abelian anyon platforms: from Majorana to Fibonacci, *Phys. Scr.* **2015**, 014006 (2015).
- [7] D. J. Clarke, J. Alicea, and K. Shtengel, *Nat. Phys.* **10**, 877 (2014).
- [8] M. Cheng, Superconducting proximity effect on the edge of fractional topological insulators, *Phys. Rev. B* **86**, 195126 (2012).
- [9] M. Burrello, B. van Heck, and E. Cobanera, Topological phases in two-dimensional arrays of parafermionic zero modes, *Phys. Rev. B* **87**, 195422 (2013).
- [10] A. Vaezi, Fractional topological superconductor with fractionalized Majorana fermions, *Phys. Rev. B* **87**, 035132 (2013).
- [11] F. Zhang and C. L. Kane, Time-Reversal-Invariant \mathbb{Z}_4 Fractional Josephson Effect, *Phys. Rev. Lett.* **113**, 036401 (2014).
- [12] M. Cheng and R. Lutchyn, Fractional Josephson effect in number-conserving systems, *Phys. Rev. B* **92**, 134516 (2015).
- [13] Y. Kim, D. J. Clarke, and R. M. Lutchyn, Coulomb blockade in fractional topological superconductors, *Phys. Rev. B* **96**, 041123(R) (2017).
- [14] B. Beri and N. R. Cooper, Topological Kondo Effect with Majorana Fermions, *Phys. Rev. Lett.* **109**, 156803 (2012).
- [15] A. Altland and R. Egger, Multiterminal Coulomb-Majorana Junction, *Phys. Rev. Lett.* **110**, 196401 (2013).
- [16] B. Beri, Majorana-Klein Hybridization in Topological Superconductor Junctions, *Phys. Rev. Lett.* **110**, 216803 (2013).
- [17] K. Snizhko, F. Buccheri, R. Egger, and Y. Gefen, Parafermionic generalization of the topological Kondo effect, *Phys. Rev. B* **97**, 235139 (2018).
- [18] M. Gau, S. Plugge, and R. Egger, Quantum transport in coupled Majorana box systems, *Phys. Rev. B* **97**, 184506 (2018).
- [19] Y. Herasymenko, K. Snizhko, and Y. Gefen, Universal Quantum Noise in Adiabatic Pumping, *Phys. Rev. Lett.* **120**, 226802 (2018).
- [20] C. J. Pedder, T. Meng, R. P. Tiwari, and T. L. Schmidt, Missing Shapiro steps and the 8π -periodic Josephson effect in interacting helical electron systems, *Phys. Rev. B* **96**, 165429 (2017).

- [21] A. E. Svetogorov, D. Loss, and J. Klinovaja, Insulating regime of an underdamped current-biased Josephson junction supporting \mathbb{Z}_3 and \mathbb{Z}_4 parafermions, *Phys. Rev. B* **103**, L180505 (2021).
- [22] C. Nayak, S. H. Simon, A. Stern, M. Freedman, and S. Das Sarma, “Non-Abelian anyons and topological quantum computation,” *Rev. Mod. Phys.* **80**, 1083 (2008).
- [23] P. Bonderson, M. Freedman, and C. Nayak, Measurement-Only Topological Quantum Computation, *Phys. Rev. Lett.* **101**, 010501 (2008).
- [24] H. Zheng, A. D. Dua, and L. Jiang, Measurement-only topological quantum computation without forced measurements, *New J. Phys.* **18**, 123087 (2016).
- [25] A. Hutter and D. Loss, Quantum computing with parafermions, *Phys. Rev. B* **93**, 125105 (2016).
- [26] A. Dua, B. Malomed, M. Cheng, and L. Jiang, Universal quantum computing with parafermions assisted by a half-fluxon, *Phys. Rev. B* **100**, 144508 (2019).
- [27] A. Carmi, Y. Herasymenko, E. Cohen, and K. Snizhko, Bounds on nonlocal correlations in the presence of signaling and their application to topological zero modes, *New J. Phys.* **21**, 073032 (2019).
- [28] S. Groenendijk, A. Calzona, H. Tschirhart, E. G. Idrisov, and T. L. Schmidt, Parafermion braiding in fractional quantum Hall edge states with a finite chemical potential, *Phys. Rev. B* **100**, 205424 (2019).
- [29] L. A. Landau, S. Plugge, E. Sela, A. Altland, S. M. Albrecht, and R. Egger, Towards Realistic Implementations of a Majorana Surface Code, *Phys. Rev. Lett.* **116**, 050501 (2016).
- [30] C. Knapp, J. I. Väyrynen, and R. M. Lutchyn, Number-conserving analysis of measurement-based braiding with Majorana zero modes, *Phys. Rev. B* **101**, 125108 (2020).
- [31] L. Fidkowski and A. Kitaev, Effects of interactions on the topological classification of free fermion systems, *Phys. Rev. B* **81**, 134509 (2010).
- [32] A. M. Turner, F. Pollmann, and E. Berg, Topological phases of one-dimensional fermions: An entanglement point of view, *Phys. Rev. B* **83**, 075102 (2011).
- [33] X. Chen, Z.-C. Gu, and X.-G. Wen, Complete classification of one-dimensional gapped quantum phases in interacting spin systems, *Phys. Rev. B* **84**, 235128 (2011).
- [34] N. Schuch, D. Pérez-García, and I. Cirac, Classifying quantum phases using matrix product states and projected entangled pair states, *Phys. Rev. B* **84**, 165139 (2011).
- [35] L. H. Santos, Parafermions in hierarchical fractional quantum Hall states, *Phys. Rev. Research* **2**, 013232 (2020).
- [36] M. Barkeshli and X.-L. Qi, Synthetic Topological Qubits in Conventional Bilayer Quantum Hall Systems, *Phys. Rev. X* **4**, 041035 (2014).
- [37] M. Barkeshli, C.-M. Jian, and X.-L. Qi, Twist defects and projective non-Abelian braiding statistics, *Phys. Rev. B* **87**, 045130 (2013).
- [38] M. Barkeshli, Y. Oreg, and X.-L. Qi, Experimental proposal to detect topological ground state degeneracy, [arXiv:1401.3750](https://arxiv.org/abs/1401.3750).
- [39] J. Klinovaja, A. Yacoby, and D. Loss, Kramers pairs of Majorana fermions and parafermions in fractional topological insulators, *Phys. Rev. B* **90**, 155447 (2014).
- [40] C. P. Orth, R. P. Tiwari, T. Meng, and T. L. Schmidt, Non-Abelian parafermions in time-reversal-invariant interacting helical systems, *Phys. Rev. B* **91**, 081406(R) (2015).
- [41] J. Klinovaja and D. Loss, Fractional charge and spin states in topological insulator constrictions, *Phys. Rev. B* **92**, 121410(R) (2015).
- [42] Y. Peng, Y. Vinkler-Aviv, P. W. Brouwer, L. I. Glazman, and F. von Oppen, Parity Anomaly and Spin Transmutation in Quantum Spin Hall Josephson Junctions, *Phys. Rev. Lett.* **117**, 267001 (2016).
- [43] K. Laubscher, D. Loss, and J. Klinovaja, Fractional topological superconductivity and parafermion corner states, *Phys. Rev. Research* **1**, 032017(R) (2019).
- [44] C. Fleckenstein, N. T. Ziani, and B. Trauzettel, \mathbb{Z}_4 Parafermions in Weakly Interacting Superconducting Constrictions at the Helical Edge of Quantum Spin Hall Insulators, *Phys. Rev. Lett.* **122**, 066801 (2019).
- [45] P. Fendley, Parafermionic edge zero modes in \mathbb{Z}_n -invariant spin chains, *J. Stat. Mech.: Theory Exp.* (2012) P11020.
- [46] Y. Oreg, E. Sela, and A. Stern, Fractional helical liquids in quantum wires, *Phys. Rev. B* **89**, 115402 (2014).
- [47] J. Klinovaja and D. Loss, Parafermions in an Interacting Nanowire Bundle, *Phys. Rev. Lett.* **112**, 246403 (2014).
- [48] J. Klinovaja and D. Loss, Time-reversal invariant parafermions in interacting Rashba nanowires, *Phys. Rev. B* **90**, 045118 (2014).
- [49] M. Thakurathi, D. Loss, and J. Klinovaja, Floquet Majorana fermions and parafermions in driven Rashba nanowires, *Phys. Rev. B* **95**, 155407 (2017).
- [50] A. Chew, D. F. Mross, and J. Alicea, Fermionized parafermions and symmetry-enriched Majorana modes, *Phys. Rev. B* **98**, 085143 (2018).
- [51] L. Mazza, F. Iemini, M. Dalmonte, and C. Mora, Nontopological parafermions in a one-dimensional fermionic model with even multiplet pairing, *Phys. Rev. B* **98**, 201109(R) (2018).
- [52] F. Ronetti, D. Loss, and J. Klinovaja, Clock model and parafermions in Rashba nanowires, *Phys. Rev. B* **103**, 235410 (2021).
- [53] K. Snizhko, R. Egger, and Y. Gefen, Measurement and control of a Coulomb-blockaded parafermion box, *Phys. Rev. B* **97**, 081405(R) (2018).
- [54] I. E. Nielsen, K. Flensberg, R. Egger, and M. Burrello, Readout of parafermionic states by transport measurements, [arXiv:2109.02300](https://arxiv.org/abs/2109.02300).
- [55] S. Trebst, M. Troyer, Z. Wang, and A. W. W. Ludwig, A short introduction to Fibonacci anyon models, *Prog. Theor. Phys. Suppl.* **176**, 384 (2008).
- [56] E. M. Stoudenmire, D. J. Clarke, R. S. K. Mong, and J. Alicea, Assembling Fibonacci anyons from a \mathbb{Z}_3 parafermion lattice model, *Phys. Rev. B* **91**, 235112 (2015).
- [57] J. Alicea, Y. Oreg, G. Refael, F. von Oppen, and M. P. A. Fisher, Non-Abelian statistics and topological quantum information processing in 1D wire networks, *Nat. Phys.* **7**, 412 (2011).
- [58] B. van Heck, A. R. Akhmerov, F. Hassler, M. Burrello, and C. W. J. Beenakker, Coulomb-assisted braiding of Majorana fermions in a Josephson junction array, *New J. Phys.* **14**, 035019 (2012).
- [59] J. Li, T. Neupert, B. A. Bernevig, and A. Yazdani, Manipulating Majorana zero modes on atomic rings with an external magnetic field, *Nat. Commun.* **7**, 10395 (2016).
- [60] M. Trif and P. Simon, Braiding of Majorana Fermions in a Cavity, *Phys. Rev. Lett.* **122**, 236803 (2019).

- [61] M. Alvarado, A. Iks, A. Zazunov, R. Egger, and A. L. Yeyati, Boundary Green's function approach for spinful single-channel and multichannel Majorana nanowires, *Phys. Rev. B* **101**, 094511 (2020).
- [62] O. Deb, K. Sengupta, and D. Sen, Josephson junctions of multiple superconducting wires, *Phys. Rev. B* **97**, 174518 (2018).
- [63] L. Peralta Gavensky, G. Usaj, and C. A. Balseiro, Topological phase diagram of a three-terminal Josephson junction: From the conventional to the Majorana regime, *Phys. Rev. B* **100**, 014514 (2019).
- [64] J. S. Meyer and M. Houzet, Conductance quantization in topological Josephson trijunctions, *Phys. Rev. B* **103**, 174504 (2021).
- [65] T. Jonckheere, J. Rech, A. Zazunov, R. Egger, A. L. Yeyati, and T. Martin, Giant Shot Noise from Majorana Zero Modes in Topological Trijunctions, *Phys. Rev. Lett.* **122**, 097003 (2019).
- [66] X. G. Wen, Electrodynamical Properties of Gapless Edge Excitations in the Fractional Quantum Hall States, *Phys. Rev. Lett.* **64**, 2206 (1990).
- [67] Our results are also valid (qualitatively) for a trijunction comprising the boundary of spin-unpolarized $\nu = \frac{2}{3}$ QH puddles. In this case, *s*-wave superconducting segments may be employed to gap out the counterpropagating edge modes.
- [68] See Supplemental Material at <http://link.aps.org/supplemental/10.1103/PhysRevB.105.L161101> for further details.
- [69] C. Chen and F. J. Burnell, Tunable Splitting of the Ground-State Degeneracy in Quasi-One-Dimensional Parafermion Systems, *Phys. Rev. Lett.* **116**, 106405 (2016).
- [70] X.-G. Wen, Edge transport properties of the fractional quantum Hall states and weak-impurity scattering of a one-dimensional charge-density wave, *Phys. Rev. B* **44**, 5708 (1991).
- [71] T. Maciążek and A. Sawicki, Non-Abelian quantum statistics on graphs, *Commun. Math. Phys.* **371**, 921 (2019).
- [72] T. Maciążek and B. H. An, Universal properties of anyon braiding on one-dimensional wire networks, *Phys. Rev. B* **102**, 201407(R) (2020).
- [73] B. H. An and T. Maciążek, Geometric presentations of braid groups for particles on a graph, *Commun. Math. Phys.* **384**, 1109 (2021).